Available online at www.sciencedirect.com
SCIENCE DIRECT®
PERGAMON
Polyhedron 22 (2003) 1113–1121
POLYHEDRON
www.elsevier.com/locate/poly

Pd(II) and Pt(II) complexes of 2,2′-biimidazole and its *N*,*N*′-dimethyl derivative. The crystal structure of [{PtBr(DMSO)}$_2$(Me$_2$bim)] (Me$_2$bim = *N*,*N*′-dimethyl-2,2′-biimidazole)

José S. Casas [a], Alfonso Castiñeiras [a], Y. Parajó [a], Mera L. Pérez-Parallé [b], Augustin Sánchez [a], Angeles Sánchez-González [a], José Sordo [a,*]

[a] *Departamento de Química Inorgánica, Universidade de Santiago de Compostela, 15782 Santiago de Compostela, Galicia, Spain*
[b] *Departamento de Bioquímica e Bioloxía Molecular, Instituto de Acuicultura, 15782 Santiago de Compostela, Galicia, Spain*

Received 22 November 2002; accepted 29 January 2003

Abstract

The complexes [PdCl$_2$(LL)] and [PtX$_2$(LL)] [X = Cl, Br or I; LL = 2,2′-biimidazole (H$_2$bim) or *N*,*N*′-dimethyl-2,2′-biimidazole (Me$_2$bim)] were prepared and characterized spectroscopically. The effects of the chloro compounds on plasmid DNA conformation were studied by electrophoresis in agarose gels, and that of [PtCl$_2$(H$_2$bim)] on calf thymus DNA by circular dichroism spectroscopy. The observation that these effects were adversely affected by addition of DMSO (originally used with [PtCl$_2$(Me$_2$bim)], to improve its solubility) prompted a study of the solvolysis of [PtCl$_2$(H$_2$bim)] by this solvent. ^{1}H and ^{195}Pt NMR, and electrospray mass spectra, showed the solvolysis of both Pt–Cl and Pt–N bonds, the release of the ligand H$_2$bim, and the formation of several polynuclear species. X-ray diffractometry of the dinuclear Pt(I) compound [{PtBr(DMSO)}$_2$(Me$_2$bim)] showed the ligand Me$_2$bim to bridge through its non-methylated N atoms between two platinum atoms, the coordination spheres of which were each completed by a Br$^-$ ligand, the S atom of a DMSO molecule, and the other Pt atom; the Pt–Pt bond is 2.5560(9) Å in length.

Keywords: Pd(II) and Pt(II) complexes; Pt(I) complexes; 2,2′-Biimidazole; *N*,*N*′-Dimethyl-2,2′-biimidazole; Crystal structure; DNA interactions; Solvolysis by DMSO

1. Introduction

The antitumour drug *cisplatin* [1], though very successful, has side effects including nephrotoxicity, ototoxicity, myelosuppression, neurotoxicity and the induction of nausea and vomiting. To avoid these effects and achieve activity against tumour lines that are resistant to *cisplatin*, research continues on the properties of other compounds of platinum and of other metals [2]. Among compounds based on group 10 metals, the most intensively studied have been the *cis*-[PtCl$_2$L$_2$] family, where L is a ligand coordinating to the metal via N; *cisplatin* itself belongs to this family. Ligands L that form part of such compounds and in which the donor N belongs to an imidazole ring include imidazole itself [3], *N*-methylimidazole [4], 2-methylimidazole and 1,2-dimethylimidazole [5], and 2-hydroxymethylbenzimidazole [6]. Also, Krebs and co-workers recently described the preparation of complexes with ligands containing *N*-methylated imidazole rings that are linked to each other either directly or through carbinol or carbonyl groups [7,8].

In previous work in our laboratory we prepared and tested the biological activity of tin(IV) complexes of 2,2′-biimidazole (H$_2$bim) and certain of its derivatives, including *N*,*N*′-dimethyl-2,2′-biimidazole (Me$_2$bim) [9]. In the work described here we synthesized chloro complexes of these two ligands (Scheme 1) with both Pt(II) and Pd(II), and investigated their ability to interact with DNA. As an aid to interpretation of the IR spectra of the complexes we also synthesized the bromo and iodo complexes of both ligands with Pt(II), and we used X-ray diffractometry to determine the structure of crystals of [{PtBr(DMSO)}$_2$(Me$_2$bim)],

* Corresponding author. Tel.: +34-981-594-636; fax: +34-981-594-912.
E-mail address: qijsordo@usc.es (J. Sordo).

0277-5387/03/$ - see front matter © 2003 Elsevier Science Ltd. All rights reserved.
doi:10.1016/S0277-5387(03)00097-4

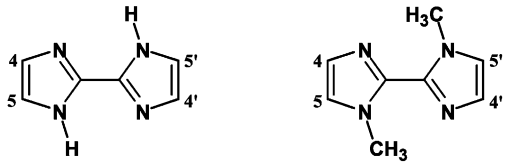

Scheme 1.

which crystallized from a DMSO solution of $[PtBr_2(Me_2bim)]$; $[\{PtBr(DMSO)\}_2(Me_2bim)]$ is the first dinuclear Pt(I) compound with a PtBrNSPt kernel to have had its structure determined.

In the experiments on interaction between the chloro complexes and DNA, the solubility of some of the compounds was improved by addition of small quantities of DMSO, which is known to influence the biological behaviour of *trans* Pt complexes and others [10]. The observation that this small concentration of DMSO significantly altered interaction with DNA led us undertake a more detailed study of the solvolysis of $[PtCl_2(H_2bim)]$ by DMSO. The main finding was evidence of significant cleavage of both Pt–Cl and Pt–N bonds.

2. Experimental

2.1. Material and methods for the synthesis of the complexes

K_2PdCl_4 (Aldrich) and K_2PtCl_4 (ABCR), were used as supplied. The ligands were prepared as described in Ref. [11]. Elemental analyses were performed with a Carlo–Erba 1108 apparatus. Melting points were determined using a Büchi apparatus. The IR spectra were recorded from KBr discs (4000–400 cm^{-1}) or polythene-sandwiched Nujol mulls (400–100 cm^{-1}) on a Bruker IFS 66V FT-IR spectrometer, on which the Raman spectra of polycrystalline samples were also recorded using an FRA-106 accessory (IR and Raman bands are reported using the following abbreviations: v = very, s = strong, m = medium, w = weak). Unless otherwise stated, ^1H and ^{13}C NMR spectra were obtained in DMF-d_7 at room temperature on a Bruker AMX300 spectrometer and referred to $SiMe_4$, and room temperature ^{195}Pt NMR spectra were obtained in the same solvent on a Bruker AMX500 spectrometer and referred to a 1 M solution of Na_2PtCl_6; chemical shifts are reported as parts per million downfield from the reference signals.

2.2. Synthesis of the complexes

2.2.1. $[PdCl_2(H_2bim)]$ (**1**)

To a solution of K_2PdCl_4 (0.35 g, 1.072 mmol) in 2 M HCl (20 ml) at 50 °C was added a suspension of H_2bim (0.15 g, 1.12 mmol) in methanol (20 ml). After 12 h stirring at room temperature the solid formed was filtered out and vacuum dried. Yield: 95% (orange solid). Found: C, 23.1; H, 1.8; N, 17.7%. Calc. for $C_6H_6N_4Cl_2Pd$: C, 23.1; H, 1.9; N, 18.0%. IR (Raman) (cm^{-1}): 335 s (343 m), 289 s (288 m), ν(Pd–Cl); 256 m (260 w), 213 s (213 m), ν(Pd–N). ^1H NMR (ppm): $\delta =$ 7.20 (d, H4/H4′), 7.53 (d, H5/H5′), 13.60 (s, vb, N–H). ^{13}C NMR (ppm): $\delta = 119.7$ (C5/C5′) 126.6 (C4/C4′) 139.6 (C2/C2′).

2.2.2. $[PdCl_2(Me_2bim)]$ (**2**)

Prepared similarly to **1** using K_2PdCl_4 (0.35 g, 1.072 mmol), 2 M HCl (17.5 ml), Me_2bim (0.178 g, 1.098 mmol), methanol (20 ml) and 24 h stirring. Yield: 86% (light orange solid). Found: C, 28.1; H, 3.0; N, 16.3%. Calc. for $C_8H_{10}N_4Cl_2Pd$: C, 28.3; H, 3.0; N, 16.5%. IR (Raman) (cm^{-1}): 348 s (318 w), 338 s, ν(Pd–Cl); 262 m (266 w), 253 w, ν(Pd–N).

2.2.3. $[PtI_2(H_2bim)]$ (**3**)

An aqueous solution of K_2PtCl_4 (0.5 g, 1.2 mmol) was treated with KI (4 g, 24 mmol) and heated at 100 °C for 5 min. H_2bim (0.18 g, 1.3 mmol) was added, and after 24 h stirring the solid product was filtered out, washed with water, ethanol and ether, and dried in vacuo. Yield: 84%. Found: C, 12.4; H, 1.0; N, 9.2%. Calc. for $C_6H_6N_4I_2Pt$: C, 12.3; H, 1.0; N, 9.6% IR (Raman) (cm^{-1}): 179 m (178 m), ν(Pt–I). ^1H NMR (ppm): $\delta =$ 7.62 (d, H4/H4′), 7.75 (d, H5/H5′), 13.68 (s, vb, N–H).

2.2.4. $[PtBr_2(H_2bim)]$ (**4**)

A suspension of $[PtI_2(H_2bim)]$ (0.391 g, 0.7 mmol) in 1 M KNO_3 (30 ml) and $AgNO_3$ (0.229 g, 2.2 mmol) were stirred for 4 h. The insoluble AgI formed was filtered out and the filtrate was treated with KBr (3.2 g, 26.8 mmol). Yield: 52% (yellow solid). Found: C, 14.9; H, 1.2; N, 11.4%. Calc. for $C_6H_6N_4Br_2Pt$: C, 14.7; H, 1.2; N, 11.4%. IR (Raman) (cm^{-1}): 220 s, 212 s (217 m), ν(Pt–Br); 228 m, 220 m, ν(Pt–N). ^1H NMR (ppm): $\delta =$ 7.50 (d, H4/H4′), 7.64 (d, H5/H5′).

2.2.5. $[PtCl_2(H_2bim)]$ (**5**)

A suspension of $[PtI_2(H_2bim)]$ (0.642 g, 1.1 mmol) in 1 M KNO_3 (30 ml) and $AgNO_3$ (0.374 g, 2.2 mmol) were stirred for 4 h. The insoluble AgI formed was filtered out and the filtrate was treated with KCl (3.3 g, 44 mmol). Yield: 37% (yellow solid). Found: C, 17.9; H, 1.3; N, 13.6%. Calc. for $C_6H_6N_4Cl_2Pt$: C, 18.0; H, 1.5; N, 14.0%. IR (Raman) (cm^{-1}): 333 s (340 m), 311 s (309 m), ν(Pt–Cl); 227 m, 218 m (218 w), ν(Pt–N). ^1H NMR

(ppm): $\delta = 7.30$ (d, H4/H4′) 7.64 (d, H5/H5′) 13.73 (s, vb, N–H). ^{13}C NMR (ppm): $\delta = 119.9$ (C5/C5′) 125.9 (C4/C4′) 141.2 (C2/C2′). ^{195}Pt NMR (ppm): $\delta = -2325$.

2.2.6. [PtI_2(Me_2bim)] (**6**)

An aqueous solution of K_2PtCl_4 (0.5 g, 1.2 mmol) was treated with KI (4 g, 24 mmol) and heated at 100 °C for 5 min. Me_2bim (0.2 g, 1.2 mmol) was added, and after stirring for 24 h, the clear brown solid obtained was filtered out, washed with water, ethanol and ether, and dried in vacuo. Yield: 64%. Found: C, 15.7; H, 1.6; N, 9.2%. Calc. for $C_8H_{10}N_4I_2Pt$: C, 15.7; H, 1.6; N, 9.2%. IR (cm^{-1}): 175 m, 171 m, ν(Pt–I); 256 m, ν(Pt–N).

2.2.7. [$PtBr_2$(Me_2bim)] (**7**)

An aqueous suspension of [PtI_2(Me_2bim)] (0.351 g, 0.5 mmol) and $AgNO_3$ (0.196 g, 1.0 mmol) were heated for 2 h and refluxed. The insoluble AgI formed was filtered out and the filtrate was treated with KBr (0.176 g, 1.5 mmol), which afforded a yellow solid. Yield: 50%. Found: C, 18.8; H, 2.1; N, 10.9%. Calc. for $C_8H_{10}N_4Br_2Pt$: C, 18.6; H, 1.9; N, 10.8%. IR (cm^{-1}): 218 s, 202 s, ν(Pt–Br); 279 m, ν(Pt–N).

A solution of this compound in DMSO afforded, after several months, plate crystals which X-ray crystallography showed to be [{PtBr(DMSO)}$_2$(Me_2bim)] (**8**).

2.2.8. [$PtCl_2$(Me_2bim)] (**9**)

Stirring a mixture of K_2PtCl_4 (0.5 g, 1.2 mmol), water (40 ml) and Me_2bim (0.195 g, 1.2 mmol) for 24 h afforded a yellow solid. Yield: 66%. Found: C, 22.0; H, 2.3; N, 12.8%. Calc. for $C_8H_{10}N_4Cl_2Pt$: C, 22.4; H, 2.3; N, 13.1%. IR (Raman) (cm^{-1}): 333 vs. (335 w), 323 sh, ν(Pt–Cl); 269 m (276 w), ν(Pt–N).

2.3. X-ray crystallography

A yellow monocrystalline plate of [{PtBr(DMSO)}$_2$(Me_2bim)] (**8**) was mounted on a glass fibre in an Enraf Nonius MACH3 automatic diffractometer [12]. Cell constants and an orientation matrix for data collection were obtained by least-squares refinement of the diffraction data from 25 reflections in the range $10.454° < \theta < 20.977°$. Data were collected at 293(2) K using Mo Kα radiation ($\lambda = 0.71073$ Å) and the ω-scan technique, and were corrected for Lorentz and polarization effects [13]. A semi-empirical absorption correction (ψ scan) was also made [14].

The structure was solved by Patterson methods [15] and subsequent difference Fourier maps, and refined on F^2 by a full-matrix least-squares procedure using anisotropic displacement parameters [16]. All hydrogen atoms were assigned in calculated positions (C–H 0.93–0.97 Å) which were refined using a riding model. Atomic scattering factors were taken from *International Tables for X-ray Crystallography* [17]. Molecular graphics were generated using PLATON-98 [18]. The crystal data, experimental details and refinement results are summarized in Table 1.

Table 1
Crystal and structure refinement data for [{PtBr(DMSO)}$_2$(Me_2bim)]

Formula weight	868.46
Temperature (K)	293(2)
Wavelength (Å)	0.71073
Crystal system	monoclinic
Space group	$C2/c$
Unit cell dimensions	
a (Å)	13.454(2)
b (Å)	14.2259(9)
c (Å)	11.1478(14)
β (°)	110.801(11)
V (Å^3)	1994.5(4)
Z	4
D_{calc} (Mg m^{-3})	2.892
Absorption coefficient (mm^{-1})	18.242
$F(0\,0\,0)$	1584
Crystal size (mm)	$0.35 \times 0.10 \times 0.10$
θ range for data collection (°)	2.50–30.39
Index ranges	$-17 \leqslant h \leqslant 19$, $-20 \leqslant k \leqslant 0$, $-15 \leqslant l \leqslant 0$
Reflections collected/unique	3156/3015 [$R_{int} = 0.0567$]
Completeness to $2\theta = 30.39$	48.1%
Absorption correction	ψ-scan
Max/min transmission	0.989, 0.775
Refinement method	full-matrix least-squares on F^2
Data/restraints/parameters	3015/0/112
Goodness-of-fit on F^2	1.094
Final R indices [$I > 2\sigma(I)$]	$R_1 = 0.0362$, $wR_2 = 0.0841$
R indices (all data)	$R_1 = 0.0840$, $wR_2 = 0.0946$
Largest difference peak and hole (e Å^{-3})	1.619 and −1.621

2.4. Drug-DNA interaction

2.4.1. Initial dissolution of drugs

Solutions of the compounds (0.1 mg/ml) were prepared at the start of each experimental series. The ligand Me_2bim and compound **1** were dissolved at 40 °C in TE buffer (10 mM Tris–HCl, 0.1 mM EDTA and 50 mM NaCl; pH 7.4); H_2bim in TE buffer containing 5% of DMSO; and compounds **2** and **9** in TE buffer containing 2.5% of DMSO. Compound **5** and *cis*-DDP were dissolved both in TE and in TE containing 2.5% of DMSO.

2.4.2. Gel electrophoresis

pUC18 DNA was isolated from *E. coli* strain DH5 by alkaline lysis [19] and was stored at −20 °C until used. After 24 or 72 h incubation of 25 μg ml^{-1} aliquots in the dark at 37 °C in drug solutions (see above) at various drug:nucleotide mole ratios r_i, the resulting products were subjected to 16 h electrophoresis at 25 V on 1.5%

agarose gels in buffer of pH 8.0 containing 40 mM Tris–acetate and 2 mM EDTA, after which the gels were stained with 0.5 μg ml^{-1} ethidium bromide.

2.4.3. Circular dichroism spectroscopy

Drug solutions (see above) were added at various drug:nucleotide mole ratios r_i to calf thymus DNA (from Sigma) in TE buffer, and the mixtures were incubated in the dark at 37 °C for 48 h. CD spectra of the products in a 1 cm rectangular quartz cell were recorded at room temperature in a JASCO J715 spectropolarimeter linked to a computer running spectral subtraction and noise reduction software. Each sample was scanned twice over the range 220–320 nm, and the CD spectra obtained from three independent replicate samples were averaged. Data are expressed as mean molar ellipticity per residue (θ) in units of $^{\circ}$ cm^2 $dmol^{-1} \times 10^3$.

2.5. Solvolysis of $[PtCl_2(H_2bim)]$ by DMSO

The solvolysis of $[PtCl_2(H_2bim)]$ by DMSO was studied by means of ^1H and ^{195}Pt NMR spectrometry and electrospray ionization mass spectrometry (ESI-MS). For ESI-MS, which was performed in positive ion mode in a Hewlett–Packard LC-MSD 1100 instrument at a cone voltage of 40 V using 49:49:2 MeCN/H_2O/HCOOH as mobile phase, 20 mg of $[PtCl_2(H_2bim)]$ was added to 0.5 ml of DMSO (previously dried over 4 Å molecular sieves) and spectra were recorded then and after 30 min and 1, 1.5, 3, 6, 24, 48 and 72 h; reported m/z values refer to the signal of greatest intensity in each isotope distribution pattern. For NMR spectrometry, which was performed at room temperature in a Bruker AMX500 apparatus, 20 mg of $[PtCl_2(H_2bim)]$/ml of DMSO-d_6 (previously dried over 4 Å molecular sieves) were used and spectra were recorded at the same times as for ESI-MS; chemical shifts are referred to $SiMe_4$ (^1H) or to a 1 M solution of Na_2PtCl_6 (^{195}Pt).

3. Results and discussion

3.1. Synthesis

The compounds $[PdCl_2(LL)]$ were prepared by adding a suspension of the appropriate ligand in methanol to a solution of K_2PdCl_4 in hot 2 M HCl. The compounds $[PtI_2(LL)]$ were obtained by adding LL to PtI_4^{2-} prepared in situ from K_2PtCl_4 and excess KI. The syntheses of the $[PtCl_2(LL)]$ (LL = H_2bim) and $[PtBr_2(LL)]$ (LL = H_2bim and Me_2bim) complexes described in Section 2 implement Dhara's method [20]; for the H_2bim complexes, to avoid the metallation of the N–H nitrogen and other side reactions during replacement of I^- with Cl^- or Br^-, we followed the procedure described for imidazole complexes [3]. We also investigated the possibility of obtaining the $[PtCl_2(LL)]$ complexes by direct reaction of the ligands with K_2PtCl_4, in spite of the risk of *trans*-$PtCl_2N_2$-kernelled polymers being generated by ligands acting in bis-monodentate bridging mode [21]; the products obtained were in fact identical to those obtained by Dhara's method, but it was the latter that gave the higher yields. All the compounds have melting points > 300 °C.

3.2. Description of the structure of $[\{PtBr(DMSO)\}_2(Me_2bim)]$

The crystal studied consists of discrete $[\{PtBr(DMSO)\}_2(Me_2bim)]$ units in which the Pt–Pt distance, 2.5560(9) Å, is close to that found in the only previously reported compound with both a Pt(I)–Pt(I) bond and an N,N' donor bridging ligand, $[Pt_2(bpy)_3](BF_4)_2$ [22], and is shorter than in other bridged [23] or unbridged [24] Pt(I)–Pt(I) compounds, and is therefore consistent with there being a single bond between the two metal centres. With this, each Pt atom is coordinated in an essentially square-planar arrangement to a Br atom, to the S atom of a DMSO molecule, to an N atom of the Me_2bim ligand, and to the other Pt atom (Fig. 1). The Pt–N bond length, 2.040(7) Å, is also close to that found in the Pt–bpy–Pt fragment of $[Pt_2(bpy)_3]^{2+}$ [22]. The Pt–S bond length, 2.194(2) Å, is close to those found in monomeric Pt(II) complexes in which the S donor atom is *trans* to N [25] or O [26] donor atoms, but is longer than the 2.169(5) Å found in

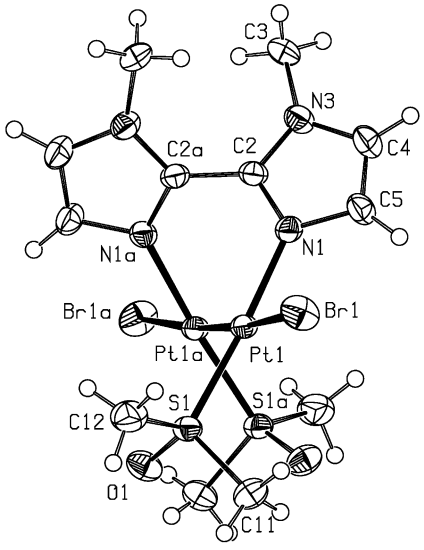

Fig. 1. The molecular structure of $[\{PtBr(DMSO)\}_2(Me_2bim)]$. Selected bond lengths (Å) and angles (°): Pt(1)–N(1) 2.040(7), Pt(1)–S(1) 2.194(2), Pt(1)–Pt(1a) 2.5560(9), Pt(1)–Br(1) 2.5837(13), N(1)–Pt(1)–S(1) 175.4(2), N(1)–Pt(1)–Pt(1a) 85.1(2), S(1)–Pt(1)–Pt(1a) 91.41(6), N(1)–Pt(1)–Br(1) 89.2(2), S(1)–Pt(1)–Br(1) 94.35(7), Pt(1a)–Pt(1)–Br(1) 174.24(3). Symmetry transformation used to generate equivalent atoms: $a = -x, y, -z+3/2$.

a dimeric Pt(I) complex in which it is *trans* to an O donor atom [27]. There are no previously reported Br–Pt(I)–Pt(I)–Br structures with which to compare the Pt–Br distance, 2.5837(13) Å, which is just slightly longer than those found in a Br–Pt(III)–Pt(III)–Br fragment [28], 2.573(1) and 2.562(1) Å. The dihedral angle between the least-squares planes defined by the atoms coordinated to each platinum is 63.70°.

The bridging biimidazole ligand is non-planar, the two practically planar imidazole rings (rms 0.0038 Å) lying at an angle of 48.3(4)° to each other (cf. 0.9(3)° in the Pt(II) compound $[PtI_2(Me_2bim)]$ [29], in which the biimidazole is bidentate). In each ring, the N(1)–C(2) and N(1)–C(5) bonds are the shortest, and their lengths, 1.332(10) and 1.378(11) Å, respectively, are similar to those found in $[PtI_2(Me_2bim)]$ [29], 1.343(12) and 1.384(12) Å, although the C(2)–N(1)–C(5) angle, 105.9(7)°, is narrower than the 107.2(8)° found in the Pt(II) compound. The bridging character of the ligand makes the C(2)–C(2a) bond longer than in the Pt(II) compound, 1.468(18) Å as against 1.413(13) Å.

3.3. Vibrational spectra

The main IR and Raman bands of the $[MX_2(LL)]$ complexes in the low-frequency range (400–100 cm^{-1}) are listed in Section 2. All the chloro complexes showed bands for the two IR active M–Cl vibrations expected for a C_{2v} MCl_2N_2 framework (A_1+B_2). Although these vibrations are also Raman-active it was not always possible to identify both Raman bands unequivocally. All these bands are located close to those found in complexes with either two *cis* monodentate *N*-donor ligands [3–5] or *N*,*N*′ bidentate ligands in which *N* and *N*′ are both incorporated in aromatic rings [30]. Identification of the ν(Pt–Cl) bands was aided by comparison with those of the $[PtI_2(LL)]$ and $[PtBr_2(LL)]$ derivatives, but identification of ν(M–N) is tentative due to the proximity of ligand bands.

The ligand bands of all the $[MX_2(LL)]$ complexes (data not shown) are slightly shifted from their positions in the spectra of the free ligands. All these shifts are in keeping with *N*,*N*′ coordination [9], all being similar to those observed for $[PtI_2(Me_2bim)]$, in which chelation by Me_2bim has been confirmed by X-ray diffractometry [29].

3.4. NMR spectra

Essential ^1H, ^{13}C and ^{195}Pt NMR data for the H_2bim complexes are listed in Section 2 (the Me_2bim complexes were too poorly soluble for satisfactory NMR spectroscopy). The ^1H NMR spectrum of the free H_2bim ligand in DMSO-d_6 shows just a single singlet at $\delta = 7.1$ ppm [9a]. No distinct N–H signal is observed, but fast exchange of this hydrogen makes all the hydrogens on the ring equivalent. This tautomerism is not observed in the solid state [31] or in DMF-d_7 solution, in which H_2bim produces three singlet signals with equal integrals at 7.02 (H4/H4′), 7.22 (H5/H5′) and 12.67 (N–H) ppm. In the ^1H NMR spectra of the $[MX_2(H_2bim)]$ complexes in DMF-d_7 the carbon-borne hydrogens appear as two doublets that have shifted downfield because of coordination to the metal. The value of $^3J_{HH}$, approximately 1.5 Hz, is similar to those found for other imidazole derivatives [32].

The poor solubility of H_2bim in DMF-d_7 makes it impossible to obtain its ^{13}C NMR spectrum in this solvent. Its ^{13}C CP/MAS spectrum [31] shows signals for carbons 4, 4′, 5 and 5′ at 129.1, 126.8, 120.8 and 118.6 ppm, respectively, but the spectrum obtained in DMSO-d_6 solution only shows a singlet at 123.4 ppm. The ^{13}C NMR spectra of the complexes in DMF-d_7 show two singlets, one for C4/C4′ and the other for C5/C5′.

The ^{195}Pt NMR signals of $[PtCl_2(H_2bim)]$ and $[PtCl_2(en)]$ appear at −2325 and −2316 ppm, respectively, showing that their Pt atoms are in similar environments and so confirming the presence of the *cis*-$PtCl_2N_2$ kernel in $[PtCl_2(H_2bim)]$.

3.5. Drug-DNA interactions

Figs. 2 and 3 show the results of gel electrophoresis of the products obtained by incubation of pUC18 plasmid DNA for 24 or 72 h with $[PdCl_2(H_2bim)]$ (**1**), $[PtCl_2(H_2bim)]$ (**5**), $[PdCl_2(Me_2bim)]$ (**2**) or $[PtCl_2(Me_2bim)]$ (**9**) at drug:nucleotide mole ratios r_i of 0.1, 0.25, 0.5 and 0.75, or with *cisplatin* at $r_i = 0.1$, 0.25 or 0.5. Neither the Pd complexes nor the ligands H_2bim and Me_2bim (results not shown) affected the mobility of either the open circular (oc) or covalently closed circular (ccc) forms of the plasmid, showing that these compounds do not modify the DNA tertiary structure, but $[PtCl_2(H_2bim)]$ and $[PtCl_2(Me_2bim)]$ did. Like *cisplatin* [33], though to a lesser extent, $[PtCl_2(H_2bim)]$ dose-dependently reduced the electrophoretic mobility of the ccc form (presumably due to partial uncoiling of the superhelix in the neighbourhood of sites at which the drug had bound) and increased that of the oc form (probably due to the induction of a shortening effect on the oc form). $[PtCl_2(Me_2bim)]$, too, slightly reduced the electrophoretic mobility of the ccc form, the effect increasing with increasing r_i and incubation time.

To test whether the DMSO included in the medium in same assays might have affected activity, we also assayed both $[PtCl_2(H_2bim)]$ and *cisplatin* in the presence of the same concentration of DMSO (Fig. 4). The activity of *cisplatin* was significantly reduced by DMSO when the incubation period was 24 h and less markedly when it was 48 h (data not shown) or 72 h, while that of $[PtCl_2(H_2bim)]$ was completely annulled except for a slight influence on ccc mobility after 72 h incubation. It

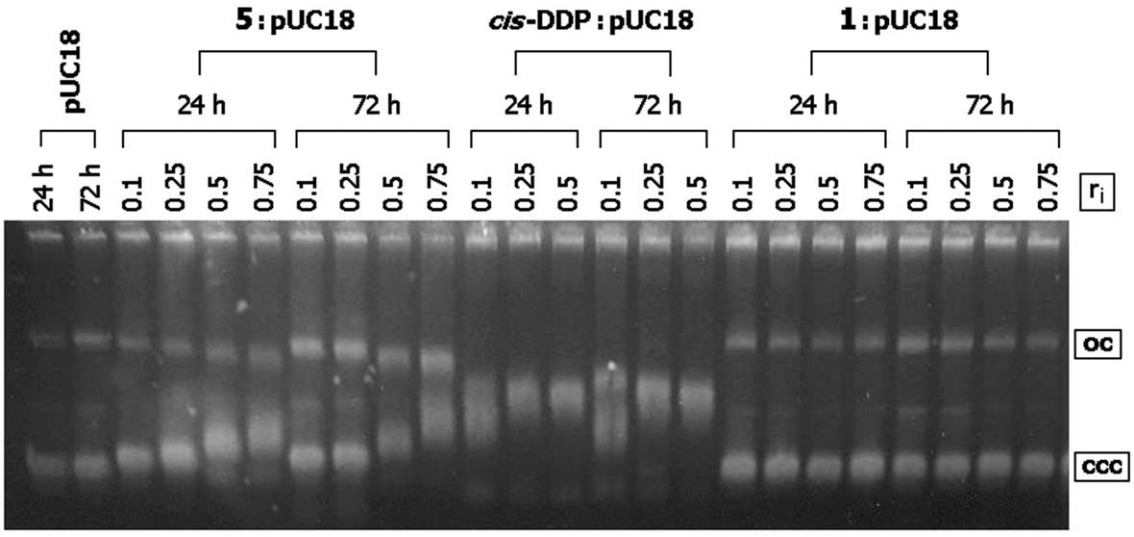

Fig. 2. Electrophoresis in agarose gel of pUC18 plasmid DNA incubated for 24 h or 72 h with compound **5** ([$PtCl_2(H_2bim)$]), compound **1** ([$PdCl_2(H_2bim)$]) or *cis*-DDP (*cis*-[$PtCl_2(NH_3)_2$]).

was concluded that DMSO converted the complex [$PtCl_2(H_2bim)$] into forms with little or no ability to modify the DNA tertiary structure.

To investigate the interaction of [$PtCl_2(H_2bim)$] with calf thymus DNA, we recorded the CD spectra of the products of their incubation together for 48 h in the presence and absence of DMSO. In the absence of DMSO, the band at 275.5 nm in the spectrum of DNA underwent a slight bathochromic shift, and increasing the concentration of [$PtCl_2(H_2bim)$] reduced both the positive ellipticity of this band and the negative ellipticity of the band at 245.5 nm (Table 2). These effects are similar to those reported for *trans*-[$PtCl_2(NH_3)_2$] (*transplatin*) [34] and for other *trans*-bifunctional adducts [35] and differ from those of *cisplatin* [34], showing that the initial *trans*/*cis* stereochemistry of this type of Pt compounds does not necessarily determine their CD-detectable effects on DNA. DMSO reduced the positive ellipticity of the CD band at 275.5 nm even in the absence of [$PtCl_2(H_2bim)$], but in the presence of

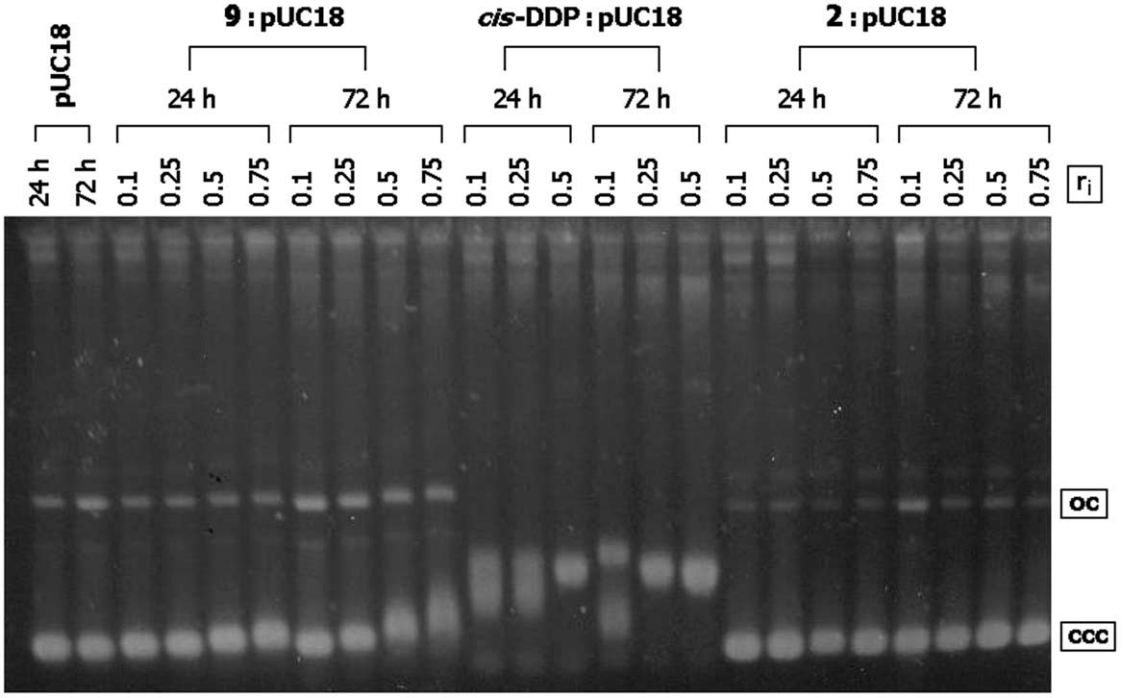

Fig. 3. Electrophoresis in agarose gel of pUC18 plasmid DNA incubated for 24 h or 72 h with compound **9** ([$PtCl_2(Me_2bim)$]) compound **2** ([$PdCl_2(Me_2bim)$]) or *cis*-DDP (*cis*-[$PtCl_2(NH_3)_2$]).

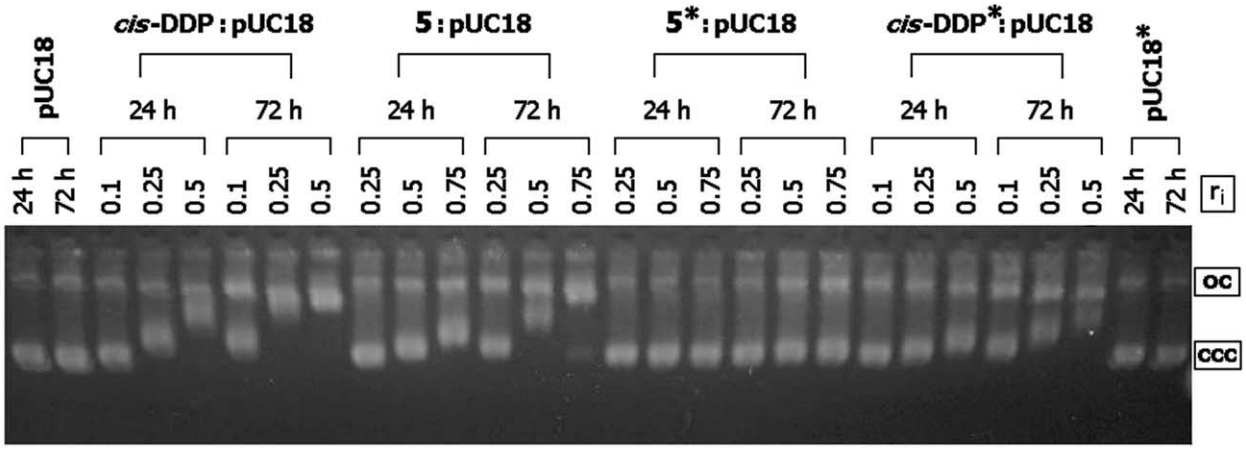

Fig. 4. Electrophoresis in agarose gel of pUC18 plasmid DNA incubated for 24 h or 72 h with compound **5** ([$PtCl_2(H_2bim)$]) or *cis*-DDP (*cis*-[$PtCl_2(NH_3)_2$]) in the presence (*) or absence of DMSO.

Table 2
CD spectral data for calf thymus DNA and its admixtures with [$PtCl_2(H_2bim)$] in various complex:nucleotide mole ratios r_i after 48 h incubation in the absence of DMSO

r_i	θ_{max} [a]	λ_{max} [b]	θ_{min} [a]	λ_{min} [b]
DNA	8.34	275.5	−9.47	245.5
0.25	7.72	277.0	−8.60	246.0
0.50	6.95	278.5	−8.45	246.0
0.75	6.40	278.5	−7.20	246.5

[a] $^{\circ}\,cm^2\,dmol^{-1} \times 10^3$.
[b] nm.

increasing concentrations of the latter ellipticity again decreased progressively (Table 3). [$PtCl_2(H_2bim)$] caused no bathochromic shift in this band when DMSO was present, but did shift the usual weak positive band at 220 nm to 225 nm.

3.6. Solvolysis of [$PtCl_2(H_2bim)$] in DMSO

To investigate the interaction of DMSO with [$PtCl_2(H_2bim)$], we monitored the evolution of solutions of the compound in DMSO by means of ESI-MS and ^1H and ^{195}Pt NMR spectroscopy.

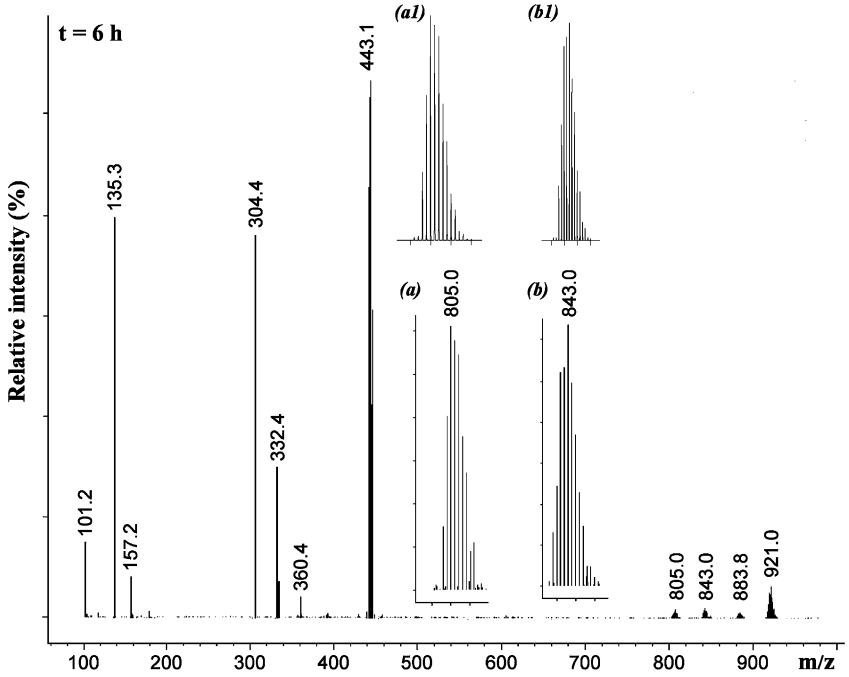

Fig. 5. Positive ion electrospray mass spectrum of [$PtCl_2(H_2bim)$] after 6 h in DMSO. The inset shows the observed (a) and calculated (a1) isotope distribution patterns of the ion $[Pt_2Cl_2(H_2bim)(Hbim)(DMSO)]^+$ ($m/z = 805.0$) and the observed (b) and calculated (b1) isotope distribution patterns of the ion $[Pt_2Cl_3(H_2bim)_2(DMSO)]^+$ ($m/z = 843.0$).

Table 3
CD spectral data for calf thymus DNA and its admixtures with $[PtCl_2(H_2bim)]$ in various complex:nucleotide mole ratios r_i after 48 h incubation in the presence of DMSO

r_i	θ_{max} [a]	λ_{max} [b]	θ_{min} [a]	λ_{min} [b]
DNA	7.60	276.0	−9.48	245.5
0.25	7.31	276.0	−8.19	245.5
0.50	7.30	276.5	−8.27	246.0
0.75	6.57	276.0	−7.43	246.0

[a] $^\circ cm^2\ dmol^{-1} \times 10^3$.
[b] nm.

Immediately following addition of $[PtCl_2(H_2bim)]$ to DMSO, or DMSO-d_6, the ^1H NMR spectrum showed signals due to this compound at 7.57 ppm (d, H5/H5′) and at 7.20 ppm (d, H4/H4′); and the ^{195}Pt NMR spectrum showed a single signal at −2319 ppm that is attributable to the same species [36]; but the ESI-MS spectrum exhibited relevant signals at $m/z = 443$ and 843, the more intense (the former) corresponding to $[PtCl(H_2bim)(DMSO)]^+$.

After 30 min, a ^{195}Pt signal corresponding to the *cis*-$PtClN_2S$ kernel of $[PtCl(H_2bim)(DMSO)]^+$ had appeared at −3161 ppm [10,37,38] and after 1 h this signal had approximately the same intensity as the $[PtCl_2(H_2bim)]$ signal. By this time (1 h), the ESI-MS signal at $m/z = 443$ was the base peak, and a signal at $m/z = 135$ corresponding to $[H_2bim+H]^+$ had appeared.

After 6 h it was possible to identify $[PtCl(H_2bim)(DMSO)]^+$ in the ^1H NMR spectrum from signals at 7.32, 7.55, 7.58 and 7.62 ppm. By this time, significant cleavage of both Pt–Cl and Pt–N bonds (interestingly the solvolysis of Pt(II) complexes of bipyridine [36] derivatives led to the complete substitution of the bypiridine ligand by DMSO with retention of *cis* configuration of two chlorides) was shown by the considerable growth of the ESI-MS signal for $[H_2bim+H]^+$ at $m/z = 135$, while the ESI-MS region for $m/z > 800$ showed not only the signal at 843 but also weak peaks at several other m/z values, including 805, 883 and 921 (Fig. 5). The signal at $m/z = 843$ is attributable to $[Pt_2Cl_3(H_2bim)_2(DMSO)]^+$, and the signal at $m/z = 805$ to $[Pt_2Cl_2(H_2bim)(Hbim)(DMSO)]^+$; possible structures for these fragments are shown in Scheme 2 (S* = DMSO). The other signals in this region may correspond to species in which the major ligand bridges between two metal centers; similar species could led to the formation of the complex studied crystallographically, $[\{PtBr(DMSO)\}_2(Me_2bim)]$, isolated from a DMSO solution of $[PtBr_2(Me_2bim)]$.

At times later than 6 h the increasing complexity of the ^1H NMR spectrum prevented identification of Pt species other than $[PtCl(H_2bim)(DMSO)]^+$, but after 24 h the release of free ligand showed up in these spectra as a singlet in the same position as in the spectrum of

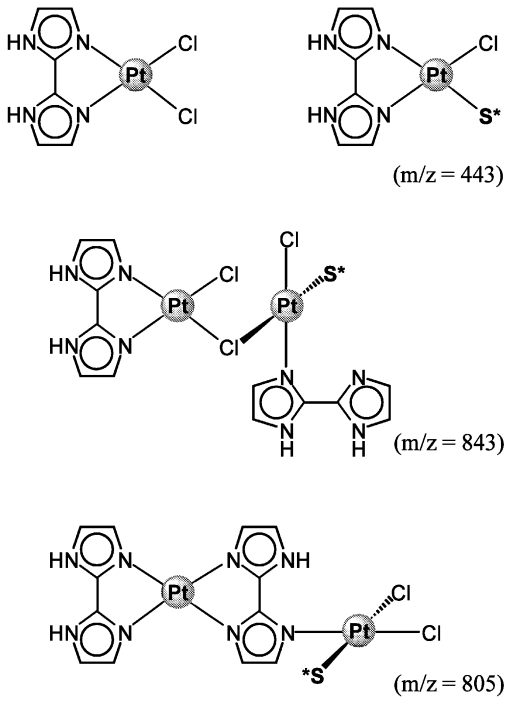

Scheme 2.

H_2bim in DMSO-d_6 + HCl, 7.60 ppm. In the ^{195}Pt NMR spectra run between 12 and 72 h after preparation of the $[PtCl_2(H_2bim)]$ solution the most intense signal was that at −3161 ppm due to the $PtClN_2S$ kernel of $[PtCl(H_2bim)(DMSO)]^+$, but it was accompanied by weak signals at −2319 ppm ($PtCl_2N_2$), −3173 ppm ($PtClN_2S$) and −2500 ppm (PtN_4) [39] and by several others between −2900 and −3000 ppm that may be due to $PtCl_2NS$ kernel [40]; these signals are in keeping with the possible structures shown in Scheme 2. The ESI-MS spectrum run after 72 h shows only signals for $[Pt_2Cl_2(H_2bim)(Hbim)(DMSO)]^+$ at $m/z = 805$, for $[PtCl(H_2bim)(DMSO)]^+$ at $m/z = 443$, and for $[H_2bim+H]^+$ at $m/z = 135$.

To sum up, the MS and ^1H and ^{195}Pt NMR results on the solvolysis of $[PtCl_2(H_2bim)]$ in DMSO confirm that cleavage of Pt–N and Pt–Cl bonds occurs to a significant extent, resulting in the release of the free ligand and allowing the formation of various mono-, di- and (possibly) polynuclear species. These solvolysis reactions are doubtless at least partly responsible for the difference between the interactions with DNA in the presence and absence of DMSO that were detected in the electrophoresis and circular dichroism experiments.

4. Supplementary material

Crystallographic data for the structure reported in this paper has been deposited with the Cambridge Crystallographic Data Center as supplementary pub-

lication number CCDC 198199. Copies of this information may be obtained free of charge from The Director, CCDC, 12 Union Road, Cambridge CB2 1EZ, UK (fax: +44-1223-336033; e-mail: deposit@ccdc.cam.ac.uk or www: http://www.ccdc.cam.ac.uk).

Acknowledgements

We thank Prof V. Moreno for valuable discussions, Prof C. Navarro-Ranninger for assistance with the circular dichroism experiments, Prof J.L. Mascareñas for granting access to the use of the JASCO J715 spectropolarimeter and the Xunta de Galicia (Spain) for financial support under projects XUGA 20318B96 and XUGA 20316B94.

References

[1] J. Reedijk, Chem. Commun. (1996) 801.
[2] (a) B.K. Keppler (Ed.), Metal Complexes in Cancer Chemotherapy, VCH, Weinheim, 1993;
(b) G. Berthon (Ed.), Handbook of Metal Ligand Interactions in Biological Fluids, vol. 2, Marcel Dekker, New York, 1995.
[3] C.G. van Kralingen, J.K. De Ridder, J. Reedijk, Inorg. Chim. Acta 36 (1979) 69.
[4] (a) C.G. van Kralingen, J. Reedijk, Inorg. Chim. Acta 30 (1978) 171;
(b) B.J. Graves, D.J. Hodgson, C.G. van Kralingen, J. Reedijk, Inorg. Chem. 17 (1978) 3007;
(c) O. Clement, A.W. Roszak, E. Buncel, J. Am. Chem. Soc. 118 (1996) 612.
[5] A.T.M. Marcelis, C.G. van Kralingen, J. Opschoor, J. Reedijk, Recueil 99 (1980) 198.
[6] F. Gümüs, Ö. Algül, J. Inorg. Biochem. 68 (1997) 71.
[7] (a) M.J. Bloemink, H. Engelking, S. Karentzopoulos, B. Krebs, J. Reedijk, Inorg. Chem. 35 (1996) 19 (and references therein);
(b) S. Karentzopoulos, H. Engelking, B. Bremer, N. Paschke, B. Krebs, Acta Crystallogr. C 53 (1997) 172.
[8] (a) M. Grehl, B. Krebs, Inorg. Chem. 33 (1994) 3877;
(b) G. Reusmann, M. Grehl, W. Reckordt, B. Krebs, Z. Anorg. Allg. Chem. 620 (1994) 199;
(c) H. Engelking, S. Karentzopoulos, G. Reusmann, B. Krebs, Chem. Ber. 127 (1994) 2355.
[9] (a) A. Sánchez-González, J.S. Casas, J. Sordo, U. Russo, M.I. Lareo, B.J. Regueiro, J. Inorg. Biochem. 39 (1990) 227;
(b) C. López, A. Sánchez González, M.E. García, J.S. Casas, J. Sordo, U. Casellato, R. Graziani, J. Organomet. Chem. 434 (1992) 261;
(c) M.P. Leal, A. Sánchez-González, M.E. García, J.S. Casas, J. Sordo, App. Organomet. Chem. 7 (1993) 421;
(d) P. Álvarez Boo, J.S. Casas, M.D. Couce, E. Freijanes, A. Furlani, V. Scarcia, J. Sordo, U. Russo, M. Varela, App. Organomet. Chem. 11 (1997) 963.
[10] (a) W.I. Sundquist, K.J. Ahmed, L. Steven Hollis, S.J. Lippard, Inorg. Chem. 26 (1987) 1524;
(b) N. Farrell, D.M. Kiley, W. Schmidt, M.P. Hacker, Inorg. Chem. 29 (1990) 397.
[11] P. Melloni, E. Dradi, W. Logemann, I. de Carneri, F. Trane, J. Med. Chem. 15 (1972) 926.
[12] B.V. Nonius, CAD4 Express Software, Ver. 5.1/1.2. Enraf Nonius, Delft, The Netherlands (1994).
[13] M. Kretschmar, GENHKL Program for the Reduction of CAD4 Diffractometer Data, University of Tübingen, Germany, 1997.
[14] A.C.T. North, D.C. Phillips, F.S. Mathews, Acta Crystallogr., Sect. A 24 (1968) 351.
[15] G.M. Sheldrick, Acta Crystallogr., Sect. A 46 (1990) 467.
[16] G.M. Sheldrick, SHELXL-97. Program for the Refinement of Crystal Structures, University of Göttingen, Germany, 1997.
[17] International Tables for X-ray Crystallography, vol. C, Kluwer Academic Publishers, Dordrecht, The Netherlands, 1995.
[18] A.L Spek, PLATON, Utrecht University, The Netherlands, 2000, http://www.cryst.chem-uu.nl/platon.
[19] T. Maniatis, E.F. Fritsch, J. Sambrook, Molecular Cloning: A Laboratory Manual, Cod Spring Harbor Laboratory Press, New York, 1989.
[20] S.C. Dhara, Ind. J. Chem. 8 (1970) 193.
[21] P. Álvarez Boo, M.D. Couce, E. Freijanes, J.S. Casas, A. Sánchez-González, J. Sordo, U. Russo, Synth. React. Inorg. Met. Org. Chem. 26 (1996) 93.
[22] G.K. Anderson, Adv. Organomet. Chem. 35 (1993) 1.
[23] A.R. Brown, Z. Guo, F.W.J. Mosselmans, S. Parsons, M. Schröder, L.J. Yellowlees, J. Am. Chem. Soc. 120 (1998) 8805.
[24] T.E. Müller, F. Ingold, S. Menzer, D.M.P. Mingos, D.J. Williams, J. Organomet. Chem. 163 (1997) 528.
[25] G.G. Arena, G. Bruno, G. De Munno, E. Rotondo, D. Dormi, F. Faraone, Inorg. Chem. 32 (1993) 1601.
[26] F.D. Rochon, P.Ch. Kong, R. Melanson, Inorg. Chim. Acta 216 (1994) 163.
[27] P. Betz, A. Bino, J. Am. Chem. Soc. 110 (1988) 602.
[28] L.S. Hollis, M.M. Roberts, S.J. Lippard, Inorg. Chem. 22 (1983) 3637.
[29] J.S. Casas, A. Castiñeiras, Y. Parajó, J. Sordo, J.M. Varela, Acta Crystallogr., Sect. C 54 (1998) 1777.
[30] S.P. Perlepes, A. Garoufis, J. Sletten, E.G. Bakalvassis, G. Plakatouras, E. Katsarou, N. Hadjiliadis, Inorg. Chim. Acta 261 (1997) 93.
[31] S. Takasu, H. Takai, T. Takagi, H. Fujisuma, Anal. Sci. 7 (1991) 845.
[32] E. Pretsch, T. Clerc, J. Seibl, W. Simon, Tablas para la elucidación estructural de compuestos orgánicos por métodos espectroscópicos, Alhambra, Spain, 1980.
[33] (a) T.S. Herman, B.A. Teicher, V. Chan, L.S. Collins, M.E. Kaufmann, C. Loh, Cancer Res. 48 (1988) 2335;
(b) G.L. Cohen, W.R. Bauer, J.K. Barton, S.J. Lippard, Science 203 (1979) 1016.
[34] J.P. Macquet, J.L. Butour, Biochimie 60 (1978) 901.
[35] G.B. Onoa, V. Moreno, J. Inorg. Biochem. 72 (1998) 141 (and references therein).
[36] J. Yoo, J. Kim, Y.S. John, Y. Do, Inorg. Chim. Acta 263 (1997) 53.
[37] J.S. Kerrison, P.J. Sadler, J. Chem. Soc., Chem. Commun. (1977) 861.
[38] T. Al Allaf, P. Castan, R. Turpin, S. Wimmer, Transition Met. Chem. 17 (1992) 579.
[39] (a) S. Komeda, H. Ohishi, H. Yamane, M. Harikawa, K. Sakaguchi, M. Chikuma, J. Chem. Soc., Dalton Trans. (1999) 2959;
(b) H. Engelking, B. Krebs, J. Chem. Soc., Dalton Trans. (1996) 2409;
(c) L.S. Hollis, S.J. Lippard, J. Am. Chem. Soc. 105 (1983) 3494;
(d) M. Roitzsch, I.B. Rother, M. Willermann, A. Erxleben, B. Costisella, B. Lippert, Inorg. Chem. 41 (2002) 5946.
[40] L.G. Marzilli, Y. Hayden, M.D. Reily, Inorg. Chem. 25 (1986) 974.